and some polymer blends. Self-similarity is attained in the regime where the structure function shows universality with time. The phase separation dynamics of the 20 wt % CTBN is reminiscent of the behavior of off-critical mixtures.

Registry No. Epon 828, 25068-38-6.

References and Notes

(1) McGarry, F. J.; Willner, A. M. *Org. Coat. Plast. Chem.* **1968**, *28*, 512.
(2) Visconti, S.; Marchessault, R. H. *Macromolecules* **1974**, *7*, 913.
(3) Boisserie, C.; Marchessault, R. H. *J. Polym. Sci., Polym. Phys. Ed.* **1977**, *15*, 1211.
(4) Gillham, J. K. *Polym. Eng. Sci.* **1979**, *19*, 676.
(5) Wang, T. T.; Zupko, H. M. *J. Appl. Polym. Sci.* **1981**, *26*, 2391.
(6) LeMay, J. D.; Kelley, F. N. *Adv. Polym. Sci.* **1986**, *78*, 115.
(7) Chan, L. C.; Gillham, J. K.; Kinloch, A. J.; Shaw, S. J. *Adv. Chem. Ser.* **1984**, *No. 208*, 235, 261.
(8) Yee, A. F.; Pearson, R. A. *J. Mater. Sci.* **1986**, *21*, 2462, 2475.
(9) Kyu, T.; Saldanha, J. M. *J. Polym. Sci., Polym. Lett. Ed.* **1988**, *26*, 33.
(10) Nojima, S.; Nose, T. *Polym. J.* **1982**, *14*, 269.
(11) Russel, T. P.; Hadziioannou, G.; Warburton, W. K. *Macromolecules* **1985**, *18*, 78.
(12) Snyder, H. L.; Meakin, P.; Reich, S. *Macromolecules* **1983**, *16*, 757.
(13) Cahn, J. W. *J. Chem. Phys.* **1965**, *42*, 93; *Trans Metall. Soc. AIME* **1968**, *242*, 1649.
(14) Hilliard, J. E. In *Phase Transformations* ASME, Oct 1968, p 497.
(15) Cook, H. E. *Acta Metall.* **1970**, *18*, 297.
(16) Hashimoto, T.; Kumaki, J.; Kawai, H. *Macromolecules* **1983**, *16*, 641.
(17) Takenaka, M.; Izumitani, T.; Hasimoto, T. *Macromolecules* **1987**, *20*, 2257.
(18) Okada, M.; Han, C. C. *J. Chem. Phys.* **1985**, *85*, 5317.
(19) Kyu, T.; Saldahna, J. M. *Macromolecules* **1988**, *21*, 1021.
(20) Bates, F. S. *Bull. Am. Phys. Soc.* **1989**, *34*, 653.
(21) Oono, Y.; Puri, S. *Phys. Rev. Lett.* **1987**, *58*, 836.
(22) Osamura, K.; Okuda, H.; Amemiya, Y.; Hashizume, H. In *Dynamics of Ordering Processes in Condensed Matter*; Komura, S., Furukawa, H. Ed.; Plenum: New York, 1989, p 273.
(23) Kumaki, J.; Hashimoto, T. *Macromolecules* **1986**, *19*, 763.
(24) Sato, T.; Han, C. C. *J. Chem. Phys.* **1988**, *88*, 2057.
(25) Kuwahara, N.; Fenly, D. V.; Tamsky, M.; Chu, B. *J. Chem. Phys.* **1970**, *55*, 1140.
(26) Chou, Y. C.; Goldburg, C. M. *Phys. Rev. A* **1981**, *24*, 3205.
(27) Nojima, S.; Ohyama, Y.; Yamaguchi, M.; Nose, T. *Polym. J.* **1982**, *14*, 907.
(28) Kyu, T.; Zhuang, P.; Mukherjee, P. *ACS Symp. Ser.* **1989**, *No. 384*, 266.
(29) Langer, J. S.; Baron, M.; Miller, H. S. *Phys. Rev. A* **1975**, *11*, 1417.
(30) Binder, K.; Stauffer, D. *Phys. Rev. Lett.* **1973**, *33*, 1006.
(31) Siggia, E. D. *Phys. Rev. A* **1979**, *20*, 595.
(32) Furukawa, H. *J. Appl. Crystallogr.* **1988**, *21*, 805.
(33) Kawasaki, K.; Ohta, T. *Prog. Theor. Phys.* **1978**, *59*, 1116.
(34) Binder, K. *Phys. Rev. B* **1977**, *15*, 4425.
(35) Snyder, H.; Meakin, P. *J. Chem. Phys.* **1986**, *85*, 6118.
(36) Katano, S.; Iizumi, M. in ref 22, p 321.
(37) Furukawa, H. *Phys. Rev. Lett.* **1979**, *43*, 136.
(38) Furukawa, H. *Physica A (Amsterdam* **1984**, *123*, 497.
(39) Komura, S.; Osamura, K.; Fujii, H.; Takeda, T. *Phys. Rev. B* **1984**, *30*, 2944; **1985**, *31*, 1278.
(40) Takahashi, M.; Horiuchi, H.; kinoshita, S.; Ohyama, Y.; Nose, T. *J. Phys. Soc. Jpn.* **1988**, *55*, 2689.
(41) Hashimoto, T.; Itakura, M.; Hasegawa, H. *J. Chem. Phys.* **1986**, *85*, 6118.
(42) Lim, D. S.; Kyu, T. *Polym. Prepr. (Am. Chem. Soc., Div. Polym. Soc.)* **1988**, *29*, 354.
(43) Furusaka, M.; Fujikawa, S.; Sakaguchi, M.; Hirano, K. in ref 22, p 281.
(44) Hashimoto, T.; Takenaka, M.; Izumitani, T. *Polym. Commun.* **1989**, *30*, 45.

Orientational Order in Aramid Solutions Determined by Diamagnetic Susceptibility and Birefringence Measurements

Stephen J. Picken

AKZO Research Laboratories Arnhem, Corporate Research, Physical Chemistry Department, P.O. Box 9300, 6800 SB Arnhem, The Netherlands. *Received March 8, 1989; Revised Manuscript Received May 18, 1989*

ABSTRACT: Diamagnetic susceptibility and birefringence measurements on lyotropic solutions of poly(4,4′-benzanilidyleneterephthalamide) in concentrated sulfuric acid are presented. Three polymer samples, with different average molecular weight $\bar{M}_w$, were used. From these experiments the orientational order parameter $\langle P_2 \rangle$ is estimated. The experimental results are explained by a mean-field-type theory similar to the Maier–Saupe model for thermotropic liquid crystals. Molecular flexibility, concentration, and molecular weight are taken into account by using simple scaling factors.

I. Introduction

In this report some diamagnetic susceptibility and birefringence measurements are described on solutions of poly(4,4′-benzanilidyleneterephthalamide) (DABT, see Figure 1) in H_2SO_4. These measurements are used to estimate the orientational order parameter $\langle P_2 \rangle$. The $\langle P_2 \rangle$ order parameter is a measurement for the degree of molecular orientation.

In a previous publication[1] measurements of the nematic–isotropic transition temperature (clearing temperature) were reported as a function of polymer concentration and average molecular weight $\bar{M}_w$. In Figure 2 the experimental results for the clearing temperature of DABT solutions in H_2SO_4 are shown. The experiments were explained by a modified Maier–Saupe (mean-field) model, where the influence of molecular flexibility and polymer concentration was included using simple scaling factors in the strength of the potential. The model will be summarized in some detail.

The experiments described here can be explained by using the same model. The plan of this paper is as fol-

0024-9297/90/2223-0464$02.50/0

PPTA

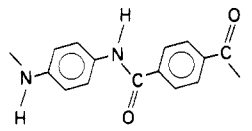

DABT

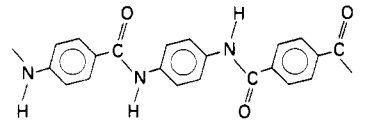

Figure 1. The aromatic polyamides (aramids) PPTA and DABT.

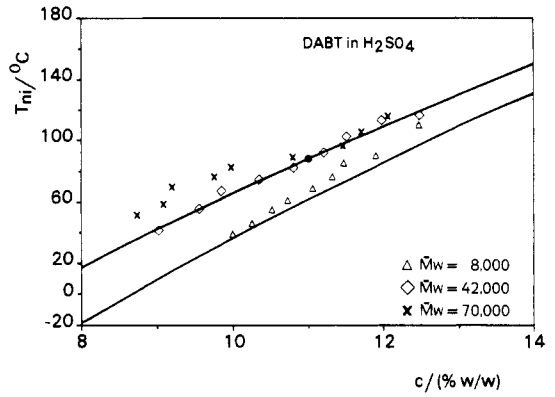

Figure 2. Clearing temperatures (T_{ni}) of DABT solutions as a function of polymer concentration and average molecular weight $\bar{M}_w$. The drawn curves correspond to the modified Maier–Saupe model described in section IV.ii. The filled circle is used to calculate ϵ^* in eq 18.

lows. First we will briefly discuss the theory behind the experimental methods to determine the temperature dependence of the $\langle P_2 \rangle$ order parameter. Next we will present the experimental results and compare them with the model mentioned before. Finally we will discuss the results and draw some conclusions.

II. Experimental Techniques To Determine the $\langle P_2 \rangle$ Order Parameter

In this section we will review the theory behind the experimental methods that are used to obtain a value for the $\langle P_2 \rangle$ order parameter. This is discussed in more detail in, e.g., ref 2.

i. Orientational Order in Liquid Crystals. The orientational order in liquid crystals is in general described by an orientational distribution function $f(\alpha,\beta,\gamma)$. This function describes the chance to find a molecule at an orientation α, β, γ with respect to the macroscopic orientation axis, commonly known as the director $\hat{n}$ (see Figure 3). The angles α, β, and γ are the Euler angles and are related to the Euler rotation matrix that completely defines the orientation of a particle in a three-dimensional space

$$\mathbf{R} = \begin{pmatrix} c\beta\, c\alpha\, c\gamma - s\alpha\, s\gamma & s\alpha\, c\beta\, c\gamma + c\alpha\, s\gamma & -s\beta\, c\gamma \\ -c\beta\, c\alpha\, s\gamma - s\alpha\, c\gamma & -c\beta\, s\alpha\, s\gamma + c\alpha\, c\gamma & s\beta\, s\gamma \\ s\beta\, c\alpha & s\beta\, s\alpha & c\beta \end{pmatrix} \quad (1)$$

where $c\alpha = \cos(\alpha)$, $s\alpha = \sin(\alpha)$, $c\beta = \cos(\beta)$, $s\beta = \sin(\beta)$, $c\gamma = \cos(\gamma)$, and $s\gamma = \sin(\gamma)$. Now we can find the relation between molecular properties and macroscopic

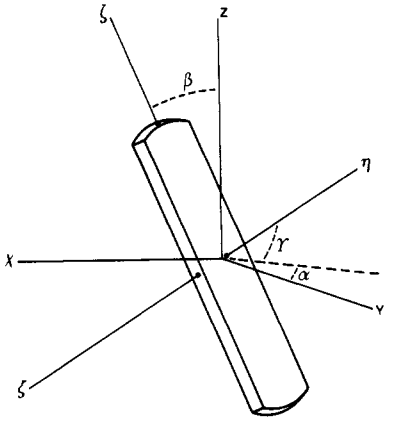

Figure 3. The Euler rotation matrix performs successive rotations around the Z, Y', and Z'' ($\equiv \zeta$) axes, respectively, over α, β, and γ radians.

ones. If a field $\vec{F}$ is applied to a liquid crystalline sample, then each molecule will find itself in a field given by $\mathbf{R}\vec{F}$.

Here the field $\vec{F}$ is either the applied magnetic or the electric field (incident light). If the molecular response to the applied field is given by the susceptibility tensor $\mathbf{k}$, then the response of one molecule is given by $\mathbf{kR}\vec{F}$. On the laboratory coordinate system the response will then be given by $\mathbf{R}^{-1}\mathbf{kR}\vec{F}$. Taking an average over all molecular orientations yields for the total response $\vec{P}$:

$$\vec{P} = N\langle \mathbf{R}^{-1}\mathbf{kR} \rangle \vec{F} \quad (2)$$

The factor N is the number of the molecules. The brackets indicate an average weighted by the orientational distribution function

$$\langle A \rangle = \int_0^{2\pi} d\alpha \int_0^{\pi} \sin(\beta)\, d\beta \int_0^{2\pi} d\gamma\, f(\alpha,\beta,\gamma) A(\alpha,\beta,\gamma) \quad (3)$$

where $A(\alpha,\beta,\gamma)$ is a molecular property on the laboratory frame. As the nematic liquid crystalline phase has cylinder symmetry, the angle α can be ignored. In addition there is uniaxial up–down symmetry so that replacing the angle β by $\pi - \beta$ will not change the physical properties of the phase.

The bulk susceptibility for the material is given by the following expression

$$\mathbf{X} = N\langle \mathbf{R}^{-1}\mathbf{kR} \rangle \quad (4)$$

This can be used to calculate the anisotropy of the susceptibility ΔX

$$\Delta X \equiv X_{\parallel} - X_{\perp} = \frac{3}{2}(X_{\parallel} - \bar{X}) \quad (5)$$

where $\bar{X} \equiv {}^1/_3(2X_{\perp} + X_{\parallel})$. It is usually assumed that the molecular susceptibility tensor can be diagonalized on a molecular coordinate system coinciding with the long molecular axis, i.e., $\mathbf{k}$ is given by

$$\mathbf{k} = \begin{pmatrix} k_{t1} & 0 & 0 \\ 0 & k_{t2} & 0 \\ 0 & 0 & k_{\parallel} \end{pmatrix} \quad (6)$$

where k_{t1} and k_{t2} are the transverse components of $\mathbf{k}$ and $k_{\parallel}$ is the component parallel to the long molecular axis. This is a reasonable assumption for many physical properties such as diamagnetic susceptibility and polarizability. In fact the molecules are often considered to be effec-

tively uniaxial, so that the two transverse components are taken to be equal.

If one now defines the following average order parameters

$$\langle P_2 \rangle = \left\langle \frac{1}{2}(3\cos^2(\beta) - 1) \right\rangle; \quad D = \left\langle \frac{3}{2}\sin^2(\beta)\cos(2\gamma) \right\rangle \tag{7}$$

one finds for the macroscopic anisotropy in the susceptibility

$$X_\parallel - X_\perp = N\Delta k\langle P_2 \rangle + \frac{1}{2}N\delta_k D \tag{8}$$

where

$$\Delta k = k_\parallel - \frac{1}{2}(k_{t1} + k_{t2}); \quad \delta_k = k_{t1} - k_{t2} \tag{9}$$

The equation for the bulk anisotropy contains two order parameters: $\langle P_2 \rangle$, the "alignment order parameter", and D, the "flatness order parameter". The first-order parameter describes the degree of alignment of the long molecular axes. The second-order parameter indicates the influence of hindered rotation, around the long molecular axis, on the anisotropy of the phase. The flatness order parameter does not imply a biaxial phase but shows that the molecules tend to deviate from the director with a preferential orientation of the aromatic rings with respect to the deviation vector.

It is not easy to determine $\langle P_2 \rangle$ and D simultaneously from anisotropy measurements. However, D is expected to be small due to rapid rotation of the molecules around their long axis, and δ_k is expected to be rather small compared to Δk. This means that the anisotropy can be approximated by

$$X_\parallel - X_\perp = N\Delta k\langle P_2 \rangle \tag{10}$$

Because the density varies very slowly with temperature, N is about constant. Approximate values for $\langle P_2 \rangle$ can be obtained from measurement of birefringence or the anisotropy of the diamagnetic susceptibility using equations similar to eq 10.

ii. Diamagnetic Susceptibility Measurements. The measurement of the diamagnetic susceptibility of a liquid crystalline material is based on the Faraday–Curie method. A sample is suspended in an inhomogeneous magnetic field, and the force is measured. This force is proportional to the diamagnetic susceptibility. Assuming that the director aligns along $\vec{B}$ and the gradient in $\vec{B}$ in along the z axis, one obtains the following expression for the force K_z:

$$K_z = \mu_0^{-1}\chi_\parallel^m m\left(\vec{B}\frac{\partial \vec{B}}{\partial z}\right) \tag{11}$$

where $\chi_\parallel^m$ is the "mass susceptibility" ($\parallel$ to $\vec{B}$), m is the mass of the sample, and μ_0 is the permittivity of the vacuum. Measurement of K_z for an anisotropic phase provides $\chi_\parallel^m$ and for an isotropic phase χ_{iso}^m. By extrapolating the isotropic values down to lower temperatures $(\chi_{iso}^m)^*$ and using the expression

$$(\chi_{iso}^m)^* = \frac{(\chi_\parallel^m + 2\chi_\perp^m)}{3} \tag{12}$$

(i.e., the change in the density at the phase transition is ignored), one can determine the anisotropy of χ as a function of temperature

$$\Delta\chi = \frac{3}{2}(\chi_\parallel^m - (\chi_{iso}^m)^*) \tag{13}$$

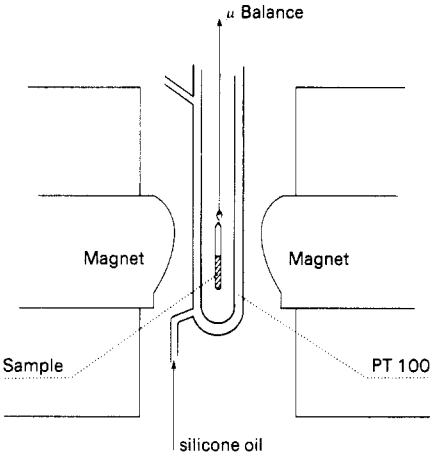

Figure 4. Schematic construction of the setup for measuring diamagnetic susceptibility.

This can now be used to estimate $\langle P_2 \rangle$ as a function of temperature, using eq 10. In Figure 4 the experimental setup for these measurements is shown. As the susceptibility is very small (about 10^{-12} m^3 mol^{-1}), the generated forces are also very small. The required accuracy of the balance is about 1 μg (= 10^{-10} N).

The assumed alignment of the director along the magnetic field lines ($\vec{n}\parallel\vec{B}$) has been reported for PBA solutions in DMA/LiCl (ref 3 and 4), using a field strength of 1.5 T or larger. The setup for measuring the diamagnetic susceptibility uses a water-cooled magnet that produces a field strength of 1.5 T so that alignment of the aramid solution should take place. Indeed, it is observed that the solution becomes more transparant, after several hours in the magnetic field, indicating a reduction in the number of disclinations in the director field.

iii. Birefringence Measurements. The index of refraction or to be more precise the permittivity can also be used to measure the orientational order in a liquid crystal. However, the interpretation of the experimental results is not so straightforward as in the case of diamagnetic susceptibility measurements. The applied electric field is substantially influenced by the polarization of the sample. (The incident light is regarded as a rapidly varying electric field, and the index of refraction is the square root of the permittivity at this frequency.)

We will not discuss the problem of the local field correction further; this has been discussed extensively in the literature (e.g. ref 2). It is found that in practice we may use an expression similar to eq 10:

$$\Delta\epsilon = \epsilon_\parallel - \epsilon_\perp = n_\parallel^2 - n_\perp^2 = \Delta\epsilon_0\langle P_2 \rangle \tag{14}$$

where $\Delta\epsilon_0$ corresponds to the anisotropy of the permittivity of a perfectly oriented sample with $\langle P_2 \rangle = 1$. Of course, $\Delta\epsilon_0$ cannot be measured so that one has to derive a reasonable value by fitting the measured values to a theoretical or empirical curve. The same applies to diamagnetic susceptibility measurements.

Several experimental methods to determine the birefringence of liquid crystals are known. With the experiments described in the following section we used an Abbe refractometer. With some experience, this allows the determination of $n_\perp$ below T_{ni} and n_{iso} above T_{ni}. The anisotropy of the permittivity can be estimated by extrapolation of the isotropic index of refraction into the nematic phase, using the relation

$$\Delta\epsilon = 3(\epsilon_{iso}^* - \epsilon_\perp) = 3(n_{iso}^{2*} - n_\perp^2) \tag{15}$$

Table I
The Studied DABT Solutions[a]

polymer	$\bar{M}_w$, amu	c, % (w/w)	T_{ni}, °C
DABT	8 000	10.5 (0.1)	55 (1)
DABT	8 000	11.4 (0.1)	85 (1)
DABT	42 000	10.8 (0.1)	87 (1)
DABT	70 000	10.3 (0.1)	76 (1)

[a] The standard deviations are given in parentheses.

The superscript asterisk indicates a value extrapolated from the isotropic phase. Here the density change at the phase transition is neglected, leading to an underestimation of $\Delta\epsilon$. From the experiments described in the next section we find that this approximation does not introduce a serious error.

III. Experimental Results

The measurements were performed on solution of DABT (Figure 1) for various values of the molecular weight $\bar{M}_w$. The polymers were dissolved in 99.8% H_2SO_4 by stirring and careful heating. The solutions that we studied are listed in Table I with the clearing temperature (at 50% phase separation) from polarization miscroscopy.

We used a Leitz Orthoplan-Pol. polarizing microscope with a Mettler FP80/82 hot-stage. The values for $\bar{M}_w$ were estimated by using a viscosity measurement at a standard polymer concentration. The calibration curve to determine the value for $\bar{M}_w$ was obtained from various experimental methods such as GPC, HP-SEC, light-scattering, and end-group analysis on PPTA (Figure 1) solutions. The molecular weight of DABT, as given in Table I, is thus only an estimate.

In ref 1 the influence of $\bar{M}_w$ and the polymer concentration on the clearing temperatures of aramid solutions was discussed. The use of DABT rather than PPTA solutions is based on the observation that DABT solutions do not crystallize, even at high ($\simeq$20% (w/w)) polymer concentration. This allows measurements to be performed on the nematic phase over a wider temperature range than is possible with PPTA solutions, leading to an improved accuracy of the extrapolations (e.g. of the isotropic index of refraction) and a wider temperature range for the $\langle P_2 \rangle$ order parameter.

Diamagnetic susceptibility measurements were only performed on the low $\bar{M}_w$ (8000 amu) and low concentration (10.5% (w/w)) DABT solution. The reason for this is that we expect a low $\bar{M}_w$ sample to be oriented more rapidly by the magnetic field than a high $\bar{M}_w$ sample. The low concentration was used to prevent polymer degradation during the rather time-consuming susceptibility measurement. This was checked afterward by using polarization microscopy, and no change in T_{ni} was found, within about 1 °C.

The setup for measuring the diamagnetic susceptibility consists of a Bruker BE15 + B MN C4 water-cooled electromagnet (H = 1.5 T) with linear field gradient polecaps (HdH/dz = constant), a Mettler BE22 + ME21 microgram balance, and a Eurotherm 140 digital thermometer. The force measurements are shown in Figure 5. We explain the observed overall slope in the measured force by the expansion of the air surrounding the sample. According to ref 12, the density of dry air at 76 cm/Hg is 1.205 mg/mL. During the diamagnetic susceptibility measurement the force increases by 0.72 mg over a temperature range from 20 to 80 °C. Using the familiar law $PV = nRT$ for an ideal gas, we calculate a change in the density of the air of 0.2 mg/mL in this temperature range.

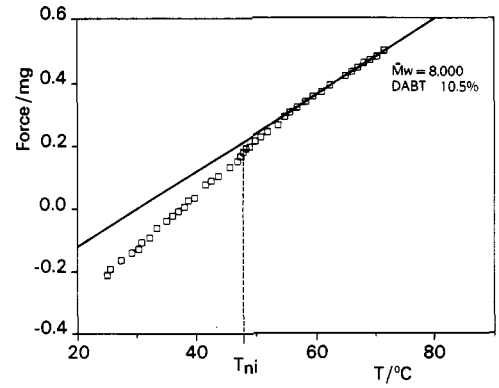

Figure 5. Measured force versus temperature. The anisotropy of the diamagnetic susceptibility is proportional to the difference between the force measured in the nematic phase and the extrapolated force from the isotropic phase (the straight line).

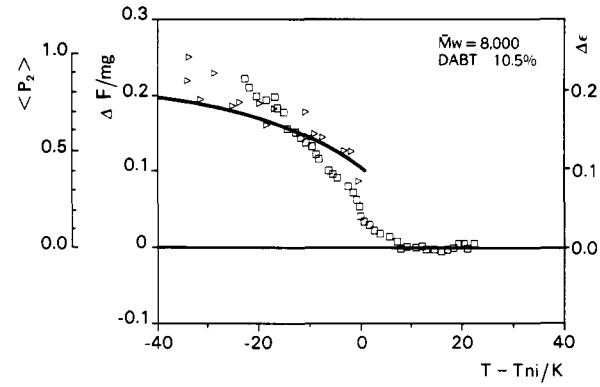

Figure 6. Force differences $\Delta F \propto \Delta\chi$ (□) and birefringence $\Delta\epsilon$ (△) values versus the relative temperature ($T - T_{ni}$). Drawn line: mean-field calculation including flexibility, as described in section IV.ii.

The measured volume of the sample was about 3.8 mL. The change in upward force (Archimedes' law) is 3.8 × 0.2 = 0.76 mg.

The difference between the measured force in the anisotropic phase and the force extrapolated from the isotropic phase is proportional to the anisotropy of the diamagnetic susceptibility. We are assuming that the density change at the phase transition is small. The results are shown in Figure 6. One unsatisfactory aspect of the measurement is that the estimated clearing temperature is less than the one determined from thermomicroscopy. This might be caused by the fact that a susceptibility measurement averages over the whole sample, whereas the presence of a certain amount of isotropic phase would not be noticed in microscopic observation.

The index of refraction, of the solutions in Table I, was measured by using an Abbe refractometer (Zeiss type B) with an Eurotherm 140 digital thermometer. The temperature was controlled by using a Tamson thermostated oil bath. In the ideal case both $n_\parallel$ and $n_\perp$ can be measured (with some practice) below the clearing temperature and of course n_{iso} above T_{ni}. Often $n_\parallel$ is very high (about 2) so that only $n_\perp$ is observed. However, with aramid solutions $n_\parallel$ can be measured as the samples contain a large amount of sulfuric acid, reducing the effective birefringence. Unfortunately the experimental error in $n_\parallel$ is rather large, so that the usual method of extrapolating the isotropic index of refraction (and using eq 15) is preferred. By performing several measurements of $n_\parallel$, it is possible to reduce the experimental error; the obtained value for the birefringence is found to be

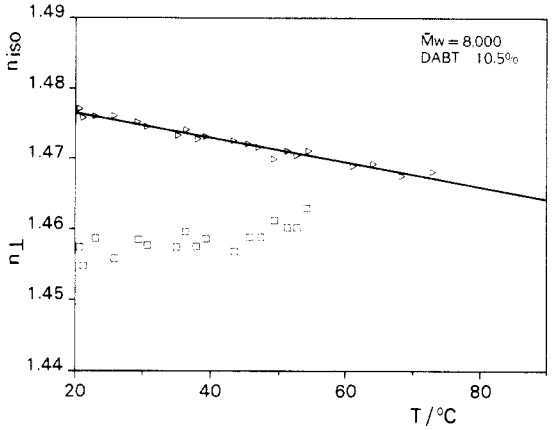

Figure 7. Index of refraction versus temperature: isotropic values (△); $n_\perp$ (□). The drawn line is the least-squares fit to the isotropic values.

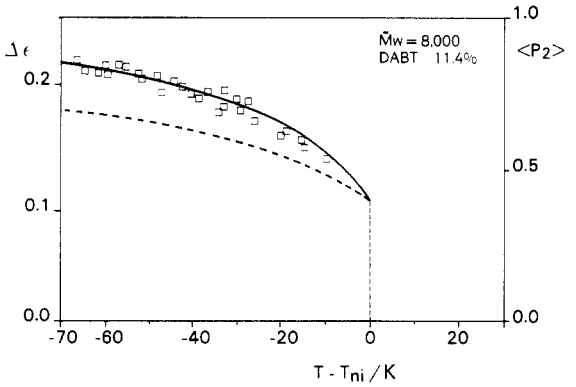

Figure 8. Anisotropy of the dielectric constant and $\langle P_2 \rangle$, as a function of the relative temperature $(T - T_{ni})$ for $\bar{M}_w$ = 8000. The drawn curve is from the present theory. The dotted curve is from the traditional Maier–Saupe model.

in good agreement with the value obtained via extrapolation of the isotropic index of refraction. This means that, surprisingly, the density change at the nematic–isotropic phase transition in DABT solutions is small.

For example, with the 10.5% (w/w) DABT solution we find the values $n_\parallel$ = 1.52 (0.01), $n_\perp$ = 1.459 (0.003), and n_{iso}* = 1.476 (0.001) at T = 24.2 °C. From this we calculate

$$(n_\parallel^2 + 2n_\perp^2)^{1/2}/3 = 1.48\ (0.01)$$

This implies that within the error bounds given there is no change in density. By averaging over all the values of $n_\parallel$ of the 10.5% (w/w) DABT solution, we conclude that the relative change in density is about 0.3 (0.1)%. This is similar to values reported for traditional low molecular weight thermotropics, about 0.3%.[5] Figure 7 shows the measured indices of refraction for the low $\bar{M}_w$ (8000 amu) and low concentration (10.5% (w/w)) DABT solution. The obtained $\Delta\epsilon$ values are also shown in Figure 6. By comparison with the results for ΔF, we find that $\Delta\chi$ and $\Delta\epsilon$ are also proportional for aramid solutions. This means that $\Delta\epsilon$ can safely be used to estimate $\langle P_2 \rangle$, without having to worry about the local field correction. The results for $\Delta\epsilon$, using the other DABT solutions mentioned in Table I, are given in Figures 8–10 (again using eq 15).

From the temperature dependence of the isotropic polarizability, we estimate the thermal expansion of the solutions and we find values between 4.5%/100 °C and 8.3%/100 °C. These values are in reasonable agreement with that of pure H_2SO_4 being 5.4%/100 °C.

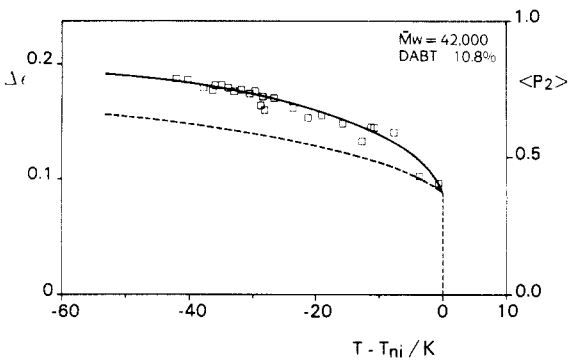

Figure 9. As in Figure 7, for $\bar{M}_w$ = 42 000.

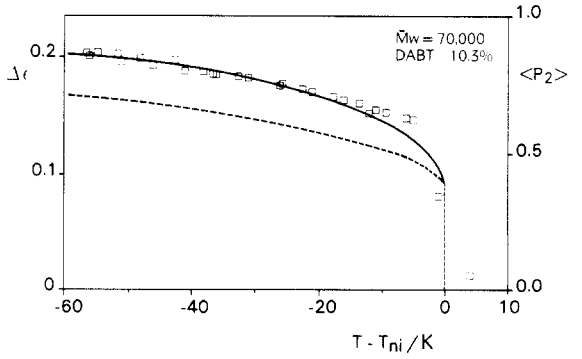

Figure 10. As in Figure 3, for $\bar{M}_w$ = 70 000.

Table II
The Constant of Proportionality $\Delta\epsilon_0$ between $\langle P_2 \rangle$ and $\Delta\epsilon$ for Various Molecular Weights of DABT[a]

M_w, amu	$\Delta\epsilon_0$	c, %	$\Delta\epsilon_0/c$
8 000	0.25 (0.02)	10.5 (0.1)	2.4 (0.2)
8 000	0.26 (0.01)	11.4 (0.1)	2.3 (0.1)
42 000	0.24 (0.01)	10.8 (0.1)	2.2 (0.1)
70 000	0.25 (0.01)	10.3 (0.1)	2.4 (0.1)

[a] The standard deviations are given in parentheses.

IV. Comparison with Theory

i. Obtaining an Estimated $\langle P_2 \rangle$ Order Parameter. By examining the measured anisotropies, one observes that the orientational order shows a temperature dependence similar to that of low molecular weight materials. To obtain reasonable estimates for the $\langle P_2 \rangle$ order parameter, there are various possible strategies. The first is to extrapolate the anisotropy down to T = 0 K so as to obtain the unknown scaling factor ($\Delta\chi_0$ or $\Delta\epsilon_0$) directly from the data. This is a somewhat risky process as one has to extrapolate over 300 K, and the data are available over about 50 K or less. Moreover, the slope of the order parameter is not expected to be constant.

Instead, to obtain $\Delta\epsilon_0$, we use the theory described in the following section. By calculating the value for $\langle P_2 \rangle$ at a specific temperature, we then calculate the corresponding value for $\Delta\epsilon_0$. Using this value, we calculate the theoretical curve $\Delta\epsilon(T)$. The used values for $\Delta\epsilon_0$ are shown in Table II. The obtained theoretical curves are shown together with the experimental data in Figures 6 and 8–10. From Table II we observe that the results for the ratio $\Delta\epsilon_0/c$ are mutually consistent. We do not give a value for $\Delta\chi_0$ as the absolute strength of the field gradient was not measured. Also the mass of the aramid solution in the quarts sample cell was not measured.

From the good agreement of the theory with the experimental data, we conclude that our model describes the temperature dependence of the $\langle P_2 \rangle$ order parameter rather well. It should be realized that apart from the

unknown birefringence at 0 K there are *no other parameters* available to "improve the fit". Of course, the experimental data has to be processed to obtain $\Delta\epsilon$ values so that there are some "hidden parameters" such as the slope and intercept of the isotropic index of refraction. We have attempted to minimize the influence of these parameters by not performing any iterations in the analysis of the data.

ii. Short Description of the Mean-Field Theory. In this section a brief description is given of a simple mean-field-type model to describe the observed behavior. The model is similar to the Maier–Saupe theory for low molecular weight thermotropic liquid crystals.[6] The present model is discussed in more detail in ref 1.

The standard Maier–Saupe model for nematic liquid crystals is based on the following mean-field potential

$$U = -\epsilon\langle P_2\rangle P_2(\cos(\beta)) \tag{16}$$

that describes the average influence of the nematic environment on the orientation of one particle. The strength of the potential is given by the parameter ϵ. The orientational order of the nematic environment is described by the order parameter $\langle P_2\rangle$. $\langle P_2\rangle$ is the average value of the second-order Legendre polynomial of cos (β): $P_2(\cos(\beta))$. In the isotropic phase $\langle P_2\rangle = 0$, while for perfect molecular alignment $\langle P_2\rangle = 1$. Solving the self-consistency equation

$$\langle P_2\rangle = \frac{\int_{-1}^{1} \mathrm{d}(\cos(\beta))\, P_2 \cos(\beta)) \exp\left(-\frac{U}{k_B T}\right)}{\int_{-1}^{1} \mathrm{d}(\cos(\beta)) \exp\left(-\frac{U}{k_B T}\right)} \tag{17}$$

and requiring that the solution corresponds to a minimum value of the free energy lead to a first-order phase transition from the nematic to the isotropic phase at $k_B T/\epsilon \simeq 0.22$.

Our extension of the Maier–Saupe model to lyotropic polymer solutions is performed by taking the influence of concentration and molecular flexibility into account by the following scaling relation

$$\epsilon = \epsilon^* c^2 L^2(T) \tag{18}$$

where c is the polymer concentration, ϵ^* is a scaling factor to be determined from experiments (using the filled circle in Figure 2), and $L(T)$ is the "contour projection length". Our choice of the exponents is based on the fact that the attractive part of the Lennard-Jones potential is proportional to $1/r^6$ which is proportional to $1/V^2$ or c^2 and that that the Maier–Saupe potential is a generalized two-particle interaction leading to a L^2 dependence.

The "contour projection length" is the average length of the projection of the wormlike chain (of finite contour length L_c) in the direction of the tangent vector at one of the end points. For low molecular weight materials where the molecules are essentially inflexible $L(T)$ is just the end-to-end distance of a molecule L_c (the contour length). For a high molecular weight material $L(T)$ corresponds to the persistence length L_p of the polymer. Using a wormlike model the following general form for the "contour projection length" is obtained:[1]

$$L(T) = L_p \frac{1 - \exp\left(-\frac{L_c T}{L_p T_p}\right)}{\frac{T}{T_p}} \tag{19}$$

where T_p is the temperature at which the persistence length is measured. Usually T_p will be approximately 20 °C (293 K). A value of 29 nm is found for the persistence length of PPTA by using dynamic light scattering methods.[7]

We observe that eq 19 corresponds to the persistence length L_p for high molecular weights ($L_c/L_p \gg 1$), with a $1/T$ temperature dependence. For low molecular weights $L(T) = L_c$ and is independent of temperature as expected. The model described here can be used to calculate the the influence of concentration and molecular weight on the clearing temperature. This is shown in Figure 2; the drawn curves are from the present theory (using eq 18 and 19 and $k_B T_{ni}/\epsilon = 0.22$). Both the effect of the concentration and of the molecular weight are in reasonable agreement with the experimental values. Of course, also the influence of temperature can be calculated for fixed values of c and $\bar{M}_w$. This leads to a calculated temperature dependence of the $\langle P_2\rangle$ order parameter. This is shown in Figures 6 and 8–10 (drawn curves). The temperature dependence of $\langle P_2\rangle$ is more pronounced in this model than in the traditional Maier–Saupe model: the molecules become more rigid with decreasing temperature, leading to higher $\langle P_2\rangle$ values.

V. Discussion

It has been shown that the orientational order parameter in aramid solutions is not unlike that of low molecular weight liquid crystals. Despite some experimental uncertainty the conclusion is that these solutions behave as thermotropic liquid crystals where the concentration only acts as a parameter determining the temperature of the nematic–isotropic phase transition. This is contrary to the models proposed by Onsager and by Flory where an anisotropic solutions of rods is governed by the axial ratio of the particles and their concentration. These models describe liquid crystals in terms of an entropy effect rather than as an energy effect. The result is that the concentration, at which the anisotropic phase is formed, is independent of temperature in these models.

Of course more advanced theories have been proposed (ref 8 and 9) that combine entropic excluded-volume terms with a Maier–Saupe potential contribution and also take molecular flexibility into account. However, the temperature dependence of the molecular flexibility is not considered. It seems to be the case that, to obtain theoretical results in agreement with experimental results (on aramids), the excluded volume contribution is of minor importance compared to the anisotropic potential. This means that these compound theories should reduce to the traditional mean-field theory.

A similar approach to the model used here is given in ref 10 and 11, where again only the Maier–Saupe potential is used to describe the formation of an anisotropic phase but where the molecular flexibility is directly included in the expression for the free energy. This means that the coupling of the molecular conformation to the molecular alignment along the director is taken into account. This is not done in the model used by us where the molecular flexibility is only solved for an isolated molecule, without considering the influence of the environment.

The question remains why the anisotropic potential seems to dominate the excluded volume term in lyotropics. This latter term should be important in solutions, where the axial ratio corresponding to the persistence length is very high (say 50) compared to low molecular weight liquid crystals (axial ratios of about 3). A possibility might be that the entropy leads to the formation

Figure 11. Schematic structure in a lyotropic phase with "blobs of dimension L_p".

of "oriented blobs"; see Figure 11. With a size on the order of L_p, the persistence length, such blobs would "line up" due to their anisotropic polarizability, meaning that the formation of long-range orientational order would be governed by a Maier-Saupe type potential. Here we are essentially postulating that the excluded volume term in the free energy only has a limited range (on the order of L_p). The excluded volume term would then only tell us something about the local molecular environment and not about long-range orientational order. It is stressed that the explanation given above is speculative and should be treated with due caution.

Acknowledgment. The author wishes to thank Dr. J. J. van Aartsen, Dr. M. G. Northolt, Dr. S. v. d. Zwaag, and Prof. dr. H. N. W. Lekkerkerker for the stimulating discussions and their continued interest in this work.

References and Notes

(1) Picken, S. J. *Macromolecules* **1989**, *22*, 1766.
(2) Vertogen, G.; de Jeu, W. H. *Thermotropic Liquid Crystals, Fundamentals*; Springer-Verlag, Berlin, 1988.
(3) Sartirana, M.; Marsano, E.; Bianchi, E.; Ciferri, A. *Macromolecules* **1986**, *19*, 1176.
(4) Takase, M.; Krigbaum, W. R. *J. Polym. Sci., Polym. Phys. Ed* **1986**, *24*, 1115.
(5) Bahadur, B. *J. Chim. Phys. Phys.-Chim. Biol.* **1976**, *73*, 255.
(6) Maier, W.; Saupe, A. *Z. Naturforsch.* **1959**, *A14*, 882; *Z. Naturforsch.* **1960**, *A15*, 287.
(7) Ying, Q.; Chu, B. *Makromol. Chem., Rapid Commun.* **1984**, *5*, 785.
(8) Khokhlov, A. R.; Semenov, A. N. *J. Stat. Phys.* **1985**, *38*(1/2), 161.
(9) Odijk, T. *Macromolecules* **1986**, *19*, 2313.
(10) Ten Bosch, A.; Maissa, P.; Sixou, P. *Phys. Lett.* **1983**, *94*(A) 298; *J. Chem. Phys.* **1983**, *79*, 3462; *J. Phys., Lett.* **1983**, *44*, L105.
(11) Warner, M.; Gunn, J. M. F.; Baumgartner, A. *J. Phys. Math. Gen.* **1985**, *18A*, 3007.
(12) *Handbook of Chemistry and Physics*, 55th ed.; CRC Press: Cleveland, 1974.

Registry No. DABT, 29153-47-7.

Turbidity of Polystyrene in Diethyl Malonate in the One-Phase Region near the Critical Solution Point

S. G. Stafford, A. C. Ploplis, and D. T. Jacobs*

Department of Physics, The College of Wooster, Wooster, Ohio 44691.
Received December 9, 1988; Revised Manuscript Received June 15, 1989

ABSTRACT: We have measured the extinction coefficient of a transmitted beam of monochromatic light through a mixture of polystyrene (molecular weight 1.02×10^5) in diethyl malonate near its upper critical solution point. The resulting turbidity was measured in a reduced temperature region, $10^{-5} < t < 10^{-1}$, where $t = (T - T_c)/T_c$ and T_c is the critical solution temperature, in two samples close to the critical composition. This polymer-solvent system near its critical point exhibits the properties of a near critical binary fluid mixture, and the turbidity can be explained by using an $n = 1$ (Ising) model. When the critical exponents ν and γ were fixed at the values predicted from renormalization group theory, the amplitude ξ_0 of the correlation length was determined to be 1.01 ± 0.08 nm, while the amplitude of the turbidity τ_0 was $(2.00 \pm 0.01) \times 10^{-4}$ cm^{-1}, which are consistent with two-scale-factor universality predictions. The turbidity far from the critical point showed an apparently constant scattering from the polymer solution. Very close to the transition temperature, the system was observed to experience a marked critical slowing with a time constant of 90 min.

Introduction

There are two critical points of interest in studying monodisperse polystyrene in a solvent.[1,2] One occurs at the coil-globule transition corresponding to the Flory Θ temperature and has been explained in terms of the $n = 0$ vector model.[2] The second is a critical solution point that produces a phase separation of the mixture into a polymer-rich phase and a polymer-poor phase, with a critical temperature and composition that depend on the system. This latter critical point has been described[2] by an $n = 1$ (Ising) model in a renormalization group theory.

Modern theories of critical solution points have been very successful in explaining a wide variety of observed phenomena in low molecular weight fluid mixtures[3,4] and, more recently, in polymer-solvent systems near their critical solution point.[5-9] In particular, the critical exponents experimentally measured in polymer-solvent sys-

0024-9297/90/2223-0470$02.50/0